Solubility of Carbon Dioxide in Aqueous Solutions of Methanol. Predictions by Molecular Simulation and Comparison with Experimental Data

Ilina Urukova, Johannes Vorholz,† and Gerd Maurer*

Lehrstuhl für Technische Thermodynamik, University of Kaiserslautern, D-67653 Kaiserslautern, Germany

Received: February 13, 2006; In Final Form: June 6, 2006

The solubility of carbon dioxide in pure methanol, and in aqueous solutions of methanol, was computed using the Gibbs ensemble Monte Carlo (GEMC) technique for 313, 354, and 395 K at pressures up to 9 MPa. Three solvent mixtures (of methanol and water) with methanol mole fractions of 10, 50, and 75 mole percent (in the gas-free solvent mixture) were studied. The Monte Carlo simulations were conducted in an isothermal−isobaric ensemble applying effective pair potentials for the pure components from literature. Common mixing rules without any adjustable binary interaction parameters were used to describe the interactions between the mixture components. Overall, a good agreement between simulation results and recently published experimental data is achieved.

1. Introduction

The solubility of gases in mixed solvents is an important factor for the design, development, and optimization of various industrial separation processes. Therefore, it has been the subject of many experimental and theoretical studies. Gas solubility data are also useful in providing essential information about the properties and structures of solutions, as well as, indirectly, in aiding the analysis of molecular interactions in solutions. Although there are some classical thermodynamic theories for the estimation of the solubility of a single gas in a solvent mixture from gas solubility data in the single solvents, there is no general method available which has been proven to provide reliable predictions for the solubility of gases in mixed solvents from pure components data alone. Molecular simulation is being considered to provide a powerful tool for the prediction of thermodynamic properties from pure component data. Here, that method is tested for the prediction of the solubility of carbon dioxide in aqueous solutions of methanol.

This contribution is an extension of a previous study on the high-pressure phase equilibrium of the ternary system carbon dioxide−methanol−water,[1] where a reasonable agreement between simulation results and experimental data was observed. Several simulation studies of methanol, aqueous methanol solutions, and binary mixtures of carbon dioxide and methanol are reported in the literature.[2−12]

The Gibbs ensemble Monte Carlo (GEMC) technique[13,14] is employed for the direct simulation of the solubility of carbon dioxide in aqueous solutions of methanol. The simulations are carried out at constant pressure and temperature. The intermolecular potentials for the pure components used are taken from the literature. The EPM2 potential model developed by Harris and Yung[15] for carbon dioxide, the simple point charge (SPC) model of Berendsen et al.[16] for water, and the model proposed by van Leeuwen and Smit[17] (LS model) for methanol are applied in all calculations. The cross interactions between unlike species are approximated by common mixing rules without any adjustable constants. The primary goal of this work is to use this method to test the capability of that technique for the prediction of gas solubility in complex systems.

This contribution presents predictions for the solubility of carbon dioxide in methanol−water mixtures with methanol concentrations (in the gas-free mixture) of 10, 50, 75, and 100 mole percent over a wide temperature and pressure range. The solubility of carbon dioxide increases with increasing methanol mole fraction in the solution. The simulation results predict this influence correctly. The simulation results are compared with recently published experimental data. The prediction results agree well with that data at low pressures, whereas somewhat larger deviations are observed at pressures near and above the critical pressure of carbon dioxide. The simulation for 354 K predicts a liquid−liquid equilibrium for the binary system carbon dioxide + methanol at pressure near the vapor pressure of pure carbon dioxide. However, such phase splits were not observed experimentally.

2. Effective Pair Potential Models

The potential model used for all three components (carbon dioxide, water, and methanol) consists of site−site pair potential functions with combine short-range Lennard-Jones and long-range Coulomb contributions. The total interaction energy u_{ij} between two molecules i and j with m and n interaction sites, respectively, is thus given by the following:

$$u_{ij} = u_{ij}^{LJ} + u_{ij}^{Coul} = \sum_{a}^{m}\sum_{b}^{n}\left\{4\epsilon_{ij}^{ab}\left[\left(\frac{\sigma_{ij}^{ab}}{r_{ij}^{ab}}\right)^{12} - \left(\frac{\sigma_{ij}^{ab}}{r_{ij}^{ab}}\right)^{6}\right] + \frac{1}{4\pi\epsilon_0}\frac{q_i^a q_j^b}{r_{ij}^{ab}}\right\} \quad (1)$$

ϵ_{ij}^{ab} and σ_{ij}^{ab} are the energy as well the size parameters of the Lennard-Jones potential between sites a and b located at molecules i and j, r_{ij}^{ab} is the site−site separation distance, q_i^a is a point charge located at site a of molecule i, q_j^b is a point charge located at site b of molecule j, and r_{ij}^{ab} in the Coulomb term denotes the distance between Coulomb site a of molecule i and Coulomb site b of molecule j. ϵ_0 (= $8.8542 \cdot 10^{-12}$ C^2 N^{-1} m^{-2}) is the permittivity of vacuum. As mentioned above,

* Corresponding author. e-mail: gmaurer@rhrk.uni-kl.de.
† Present address: Degussa AG, D-63457 Hanau-Wolfgang, Germany.

10.1021/jp060910o CCC: $33.50
Published on Web 07/13/2006

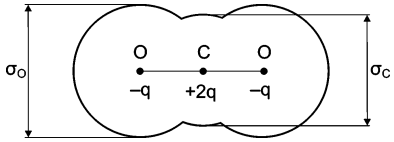

Figure 1. Schematic geometry of the EPM2 potential model for carbon dioxide.

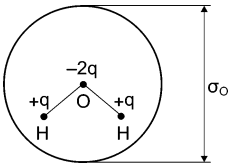

Figure 2. Schematic geometry of the SPC potential model for water.

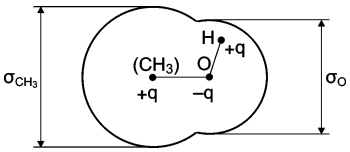

Figure 3. Schematic geometry of the LS potential model for methanol.

TABLE 1: Geometry Data and Potential Parameters for the Components Studied in This Work

carbon dioxide (EPM2, ref 15)		water (SPC, ref 16)		methanol (LS, ref 17)	
r_{C-O} (Å)	1.149	α_{HOH} (°)	109.47	$\alpha_{(CH3)OH}$ (°)	108.53
σ_O (Å)	3.033	r_{O-H} (Å)	1.00	$r_{(CH3)-O}$ (Å)	1.4246
ϵ_O/k (K)	80.507	σ_O (Å)	3.166	r_{O-H} (Å)	0.9451
σ_C (Å)	2.757	ϵ_O/k (K)	78.197	σ_O (Å)	3.030
ϵ_C/k (K)	28.129	q_O (e)	−0.82	ϵ_O/k (K)	86.500
q_O (e)	−0.3256	q_H (e)	0.41	σ_{CH3} (Å)	3.740
q_C (e)	0.6512			ϵ_{CH3}/k (K)	105.200
				q_O (e)	−0.700
				q_{CH3} (e)	0.265
				q_H (e)	0.435

the EPM2 model of Harris and Yung[15] is used for carbon dioxide, whereas the SPC model of Berendsen et al.[16] is used for water, and the LS model proposed by van Leeuwen and Smit[17] is used for methanol. Figures 1−3 show the geometry of these potentials. The potential parameters and charge distributions are given in Table 1. The same potential models were previously used for phase equilibrium predictions at high pressures,[1] where a reasonable agreement with experimental data was found. For carbon dioxide, there are three interaction sites located on the carbon atom and both oxygen atoms, respectively. Each site is the center of a Lennard-Jones potential with an embedded central point charge. Parameter values were optimized for the reproduction of the vapor−liquid equilibrium of pure carbon dioxide.[15] The extensive simulation study of Vorholz et al.[18] has shown that the phase envelope as well as the density on some supercritical isotherms are reproduced well with the re-scaled parameters taken from Harris and Yung.[15] The SPC potential models water as a Lennard-Jones center on the oxygen atom and a single negative point charge combined with two positive point charges which represent the hydrogen atoms. The potential parameters were adjusted to reproduce the density, the internal energy, and the structure of liquid water at 300 K and pressures close to zero. The LS model represents a methanol molecule as a combination of two Lennard-Jones sites (one for the methyl group and one for the oxygen atom) with three partial point charges. The point charges are located on the Lennard-Jones centers (i.e., the methyl group and the oxygen atom) and on the hydroxyl proton (H). Model parameters were fitted to simultaneously describe the density of liquid methanol (at 400 K and at 450 K), the vapor−liquid coexistence curve, and some other related thermodynamic properties of pure methanol.[17]

The Lennard-Jones interactions between unlike sites ($i \neq j$) within the same or in different molecules are calculated by the standard Lorentz−Berthelot mixing rules, i.e., the cross Lennard-Jones size parameter σ_{ij} is determined as the arithmetic mean of σ_{ii} and σ_{jj}:

$$\sigma_{ij} = \frac{\sigma_{ii} + \sigma_{jj}}{2} \tag{2}$$

except for carbon dioxide where the geometric mean is used:[15]

$$\sigma_{ij} = \sqrt{\sigma_{ii}\sigma_{jj}} \tag{3}$$

The cross energy well depth ϵ_{ij} is always calculated as the geometric mean of the energy parameters ϵ_{ii} and ϵ_{jj}:

$$\epsilon_{ij} = \sqrt{\epsilon_{ii}\epsilon_{jj}} \tag{4}$$

No adjustable binary interaction parameters were used.

It should be mentioned that other potential models for carbon dioxide, methanol, and water (e.g., based on an exp. 6 + Coulomb functional, see, for example, Errington and Panagiotopoulos[19] and Potoff et al.[2]) are available. However, the models studied in the present work are still of great interest, especially since they were already successfully employed in phase equilibria simulations of mixtures (e.g., Kristóf et al.,[1] Vorholz et al.[18]).

3. Molecular Simulation Details

All simulations were performed using the Gibbs ensemble Monte Carlo technique in the isothermal−isobaric ensemble[14] (NpT-GEMC simulations). This method is based on performing calculations in two separate microscopic regions (subsystems) within the bulk phases, away from the interface. Both subsystems are internally in thermodynamic equilibrium as well as in equilibrium with each other. Equilibrium (i.e., equality of temperature, pressure, and chemical potentials in the two regions) is obtained by displacements of particles within the subsystems, volume fluctuations, and particle transfers between the two phases. These displacements are commonly called "moves". Each type of move is selected randomly, but with a fixed probability. The efficiency of the transfer steps was increased by multiple trial insertions of the particles, and selection of the energetically most favorable position through its corrected statistical weight (for details, cf. Vorholz et al.[18]). The probability of the transfer moves was varied between 10% and 35% in the simulations. Each attempt to transfer a molecule from one box to another comprised between 10 and 20 trial insertions (depending on the system's density). The probability of volume changes was kept at 1%. The probability of particle displacements (translations or rotations) within the subsystems ranged from 64 to 89%. The same number of attempts for translational and rotational moves was applied. All simulations were carried out using a total of 600 molecules. The number of gas molecules was varied between 150 and 200, depending on the pressure. Short-range contributions to the system's energy from the Lennard-Jones potentials were computed with a method proposed by Theodorou and Suter.[20] Long-range Coulombic interactions were considered by applying the Ewald summation method within vacuum boundary conditions.[21,22] Initial configurations were generated randomly. The system was equilibrated in two steps. For the first 5 million cycles, the

TABLE 2: Simulation Results for the Solubility of Carbon Dioxide in (Water + Methanol) and Comparison with a Correlation for the Experimental Data of Xia et al.[24] given by Pérez-Salado Kamps[23]

T (K)	p (MPa)	$\tilde{x}_M$ (mol/mol)	$\Delta\tilde{x}_M$ (mol/mol)	$m_{CO_2}^{(cor)}$ (mol/kg)	$m_{CO_2}^{(sim)}$ (mol/kg)	$\Delta m_{CO_2}^{(sim)}$ (mol/kg)	$m_{CO_2}^{(sim)} - m_{CO_2}^{(cor)}$ (mol/kg)	$\overline{N_M^{II}}$ (−)	$\overline{N_{H_2O}^{II}}$ (−)	$\overline{N_{CO_2}^{II}}$ (−)
313.75	1.0	0.0998	0.0012	0.257	0.204	0.071	−0.053	1.2	1.1	147
313.75	3.0	0.1013	0.0002	0.694	0.679	0.168	−0.015	0.29	0.40	142
313.75	5.0	0.1013	0.0004	1.030	1.013	0.160	−0.017	0.28	0.20	139
313.75	7.0	0.1013	0.0003	1.280	1.234	0.120	−0.046	0.26	0.18	137
313.75	1.0	0.4979	0.0008	0.569	0.512	0.096	−0.057	2.7	0.86	144
313.75	3.0	0.4993	0.0006	1.809	1.850	0.284	0.041	0.97	0.39	129
313.75	5.0	0.4994	0.0004	3.163	3.161	0.361	−0.001	0.71	0.15	114
313.75	7.0	0.4996	0.0003	4.658	4.643	0.188	−0.015	0.51	0.12	98
313.75	1.0	0.7477	0.0009	0.971	0.954	0.112	−0.017	3.7	0.54	138
313.75	2.0	0.7525	0.0008	2.121	1.930	0.107	−0.191	2.2	0.22	125
313.75	3.0	0.7486	0.0004	3.398	3.397	0.173	−0.001	4.1	1.2	107
313.75	4.0	0.7497	0.0001	4.926	5.056	0.362	0.130	0.91	0.14	142
313.75	5.0	0.7497	0.0002	6.756	6.874	0.462	0.118	0.88	0.13	122
313.75	6.0	0.7498	0.0001	9.059	9.054	0.352	−0.005	0.49	0.08	97
313.75	7.0	0.7512	0.0006	12.225	12.422	0.654	0.197	1.3	0.33	127
313.75	1.0	1.0	0.0	1.683	1.563	0.081	−0.120	6.6		135
313.75	1.5	1.0	0.0	2.656	2.484	0.213	−0.172	2.5		116
313.75	2.0	1.0	0.0	3.711	3.723	0.209	0.012	2.1		114
313.75	3.0	1.0	0.0	6.128	6.033	0.647	−0.095	1.8		63
313.75	4.0	1.0	0.0	9.109	8.631	0.476	−0.478	0.23		26
313.75	5.0	1.0	0.0	12.983	10.947	0.640	−2.035	1.1		128
354.35	1.0	0.0953	0.0005	0.143	0.132	0.085	−0.011	4.1	8.1	147
354.35	3.0	0.0980	0.0018	0.426	0.406	0.124	−0.020	2.2	3.2	144
354.35	5.0	0.0982	0.0030	0.670	0.675	0.237	0.005	2.0	1.9	142
354.35	7.0	0.1012	0.0006	0.887	1.019	0.157	0.132	0.35	0.78	139
354.35	9.0	0.1002	0.0009	1.064	1.262	0.158	0.199	0.88	1.0	137
354.35	1.0	0.4862	0.0045	0.330	0.312	0.133	−0.018	20	8.8	147
354.35	3.0	0.4945	0.0013	1.151	1.168	0.114	0.017	7.6	2.8	137
354.35	5.0	0.4974	0.0010	2.039	2.131	0.452	0.092	3.5	1.2	126
354.35	7.0	0.4981	0.0007	2.996	2.829	0.374	−0.167	2.7	0.99	119
354.35	8.0	0.4978	0.0007	3.503	3.866	0.147	0.363	2.9	0.90	107
354.35	1.0	0.7445	0.0042	0.536	0.583	0.049	0.047	25	5.8	143
354.35	2.0	0.7515	0.0016	1.235	1.238	0.080	0.003	11	2.4	135
354.35	3.0	0.7463	0.0011	1.961	1.967	0.138	0.007	8.2	1.2	126
354.35	4.0	0.7541	0.0002	2.803	2.782	0.279	−0.020	5.4	0.89	115
354.35	5.0	0.7473	0.0006	3.641	3.479	0.435	−0.162	4.9	0.72	106
354.35	6.0	0.7572	0.0003	4.706	4.604	0.414	−0.102	2.7	0.55	91
354.35	7.0	0.7570	0.0007	5.819	5.799	0.576	−0.020	2.9	0.45	74
354.35	8.0	0.7576	0.0001	7.104	7.913	0.327	0.809	1.3	0.31	49
354.35	1.0	1.0	0.0	0.812	0.859	0.079	0.048	27	−	138
354.35	1.5	1.0	0.0	1.340	1.252	0.174	−0.088	21		133
354.35	2.0	1.0	0.0	1.891	1.938	0.105	0.047	16		123
354.35	2.5	1.0	0.0	2.468	2.393	0.106	−0.074	11		116
354.35	3.0	1.0	0.0	3.071	3.065	0.298	−0.006	9.7		107
354.35	4.0	1.0	0.0	4.368	4.043	0.192	−0.325	6.3		94
354.35	5.0	1.0	0.0	5.806	5.788	0.450	−0.018	3.8		67
354.35	6.0	1.0	0.0	7.420	7.315	0.480	−0.105	2.2		46
354.35	7.0	1.0	0.0	9.261	10.001	0.325	0.740	69		26
395.0	1.0	0.0681	0.0023	0.083	0.074	0.016	−0.010	21	58	148
395.0	3.0	0.0886	0.0026	0.319	0.308	0.097	−0.011	8.0	15	146
395.0	5.0	0.0933	0.0014	0.543	0.453	0.111	−0.090	5.2	8.8	145
395.0	7.0	0.0954	0.0018	0.751	0.799	0.149	0.049	3.9	6.2	142
395.0	9.0	0.0978	0.0021	0.947	1.028	0.070	0.081	2.9	7.1	140
395.0	1.0	0.4637	0.0113	0.155	0.209	0.065	0.054	67	43	148
395.0	3.0	0.4740	0.0066	0.814	0.828	0.132	0.014	33	12	142
395.0	5.0	0.4879	0.0032	1.563	1.594	0.170	0.031	16	5.7	133
395.0	7.0	0.4934	0.0025	2.377	2.511	0.233	0.134	11	5.2	123
395.0	9.0	0.4967	0.0019	3.272	3.475	0.193	0.202	5.8	2.9	112
395.0	1.0	0.7406	0.0051	0.208	0.302	0.020	0.094	99	30	147
395.0	2.0	0.7348	0.0029	0.728	0.758	0.165	0.031	60	13	142
395.0	3.0	0.7451	0.0053	1.293	1.306	0.134	0.013	38	6.7	135
395.0	4.0	0.7469	0.0030	1.885	1.892	0.270	0.008	28	4.4	127
395.0	5.0	0.7627	0.0015	2.569	2.538	0.448	−0.031	22	4.5	120
395.0	6.0	0.7446	0.0027	3.159	3.139	0.581	−0.020	17	3.3	111
395.0	7.0	0.7637	0.0025	3.987	3.904	0.409	−0.082	16	3.1	102
395.0	1.0	1.0	0.0	0.229	0.299	0.049	0.070	281		148
395.0	1.5	1.0	0.0	0.592	0.587	0.068	−0.005	156		144
395.0	2.0	1.0	0.0	0.968	0.905	0.108	0.064	104		140
395.0	2.5	1.0	0.0	1.357	1.337	0.132	−0.020	64		133
395.0	3.0	1.0	0.0	1.760	1.722	0.132	−0.038	49		128
395.0	3.5	1.0	0.0	2.178	2.110	0.285	−0.068	43		122

TABLE 2 (Continued)

T (K)	p (MPa)	$\tilde{x}_M$ (mol/mol)	$\Delta\tilde{x}_M$ (mol/mol)	$m_{CO_2}^{(cor)}$ (mol/kg)	$m_{CO_2}^{(sim)}$ (mol/kg)	$\Delta m_{CO_2}^{(sim)}$ (mol/kg)	$m_{CO_2}^{(sim)} - m_{CO_2}^{(cor)}$ (mol/kg)	$\overline{N_M^{II}}$ (−)	$\overline{N_{H_2O}^{II}}$ (−)	$\overline{N_{CO_2}^{II}}$ (−)
395.0	4.0	1.0	0.0	2.611	2.490	0.197	−0.121	35		117
395.0	5.0	1.0	0.0	3.527	3.441	0.365	−0.086	26		103
395.0	6.0	1.0	0.0	4.518	4.625	0.344	0.108	17		83
395.0	7.0	1.0	0.0	5.594	5.279	0.322	−0.314	17		79

probability of transfer of a methanol molecule between the two phases was set to zero, whereas for water and carbon dioxide, a phase transfer was possible. This procedure reduces the number of cycles for equilibration while it keeps the composition of the gas-free solvent mixture close to that of the "feed". In the second step of the equilibration process (typically in about 5−10 million cycles), phase transfers were allowed for all components in the isothermal−isobaric ensemble. At the end of that step, equilibrium was achieved and the so-called "production phase" started. In the production phase another 10−40 million cycles were carried out to accumulate the ensemble averages of the desired quantities, and to estimate the statistical uncertainties of the simulation results by the block averaging technique. Typically a block consists of about 1−2 million cycles. The thermodynamic properties of interest were calculated as block averages. The statistical uncertainty of a simulation result is approximated by the standard deviation from the corresponding ensemble average. For example, the residual internal energy U is calculated as follows:

$$U = \langle \sum_{i<j} u_{ij} \rangle \tag{5}$$

where u_{ij} refers to the intermolecular interaction energy between two molecules i and j.

The mass-related density ρ is calculated as the following:

$$\rho = \left\langle \frac{\sum_j N_j M_j}{N_A V} \right\rangle \tag{6}$$

Here, N_j and V stand for the number of molecules of component j and the volume in the respective phase. M_j is the molecular mass of component j, and N_A is Avogadro's number. The mole fractions of component i in the liquid and in the gas phase were calculated as follows:

$$x_i, y_i = \left\langle \frac{N_i}{\sum_j N_j} \right\rangle \tag{7}$$

The angular brackets $\langle\ \rangle$ in eqs 5−7 denote an ensemble average. The liquid-phase mole fraction (x_i) was converted to molality (m_i), which is the number of moles of dissolved gas per kilogram of solvent:

$$m_i = \frac{1000\, x_i}{(1 - x_i) M^*} \tag{8}$$

where M^* is the relative molar mass of the gas-free solvent mixture:

$$M^* = \tilde{x}_W M_W + \tilde{x}_M M_M \tag{9}$$

M_W is the molecular mass of water, M_M is the molecular mass of methanol, $\tilde{x}_W$ and $\tilde{x}_M$ are the mole fractions of water and methanol, respectively, in the gas-free solvent mixture.

4. Simulation Results and Discussion

Simulation results (using the same potentials as in the present work) for the solubility of carbon dioxide in pure water and for the high-pressure multiphase equilibrium of the system (carbon dioxide + methanol + water) have been reported by Vorholz et al.[18] and Kristóf et al.[1] In the present study, the solubility of carbon dioxide in pure methanol and in aqueous solutions of methanol was simulated for three temperatures (313.75, 354.35, and 395.0 K) and for pressures up to 9.0 MPa. The simulation results are summarized and compared with the experimental data from Xia et al.[24] in Table 2. That comparison is performed using a correlation by Pérez-Salado Kamps[23] which describes the experimental data of Xia et al.[24] within the experimental uncertainties. Table 2 also gives the absolute statistical uncertainty in the mole fraction of methanol in the gas-free solvent mixture ($\Delta\tilde{x}_M$) as well as in the molality of carbon dioxide ($\Delta m_{CO_2}^{(sim)}$) and the average number of methanol ($\overline{N_M^{II}}$), water ($\overline{N_{H_2O}^{II}}$), and carbon dioxide ($\overline{N_{CO_2}^{II}}$) molecules in the vapor phase. The simulation results for the density (ρ^I and ρ^{II}) and residual contribution to the internal energy (u^I and u^{II}) of the coexisting liquid and vapor phases are given in Table 3. The statistical uncertainty of the simulation results for the solubility of carbon dioxide is typically between 5 and 15%, in a few cases it is below 5% and beyond 30%. The relative average deviation between experiment and simulation for the liquid-phase molality of carbon dioxide is 8.7% at $\overline{\tilde{x}_M} = 0.1$, 6.5% at $\overline{\tilde{x}_M} = 0.5$, 4.5% at $\overline{\tilde{x}_M} = 0.75$, and 5.3% at $\overline{\tilde{x}_M} = 1.0$. That means that with the exception of some single data points at pressures near and above the critical pressure of carbon dioxide ($p_C = 7.38$ MPa), the difference between the experimental data and the simulation result for the liquid-phase molality of carbon dioxide is smaller than the statistical uncertainties of the simulation results and in general a good agreement between predictions and experiments for the solubility of carbon dioxide is observed. However, it should also be mentioned that at 354.35 K the simulation results for the binary system carbon dioxide + methanol result in a liquid−liquid equilibrium starting near the critical pressure of carbon dioxide. Such phase splits have not been observed experimentally.

The differences between the experimental results and the simulation results are discussed in more detail in Figures 4−7. Figure 4 shows plots of the total pressure versus the molality of carbon dioxide in the liquid phase for all investigated mixture compositions at 313.75, 354.35, and 395.0 K, respectively. As expected, the solubility of carbon dioxide in (water + methanol) increases with increasing mole fraction of methanol in the solvent mixture, as carbon dioxide is more soluble in methanol than in water. The simulation results predict this behavior. The predicted results are more accurate at lower pressures and low temperatures than at higher pressures and higher temperatures. For example, the average relative deviation between the simulation results and the experimental data for the molality of

TABLE 3: Simulation Results for the Densities and the Residual Part of the Internal Energy in the System Carbon Dioxide−Methanol−Water[a]

T (K)	$\tilde{x}_M$ (mol/mol)	p (MPa)	ρ^I (kg/m^3)	$\Delta\rho^I$ (kg/m^3)	ρ^{II} (kg/m^3)	$\Delta\rho^{II}$ (kg/m^3)	u^I (kJ/kg)	Δu^I (kJ/kg)	u^{II} (kJ/kg)	Δu^{II} (kJ/kg)	state
313.75	0.0998	1.0	933.0	9.8	17.3	0.1	−2074	15.9	−4.9	0.1	VLE
	0.1013	3.0	936.2	6.1	57.1	0.3	−2032	23.8	−16.4	0.3	VLE
	0.1013	5.0	938.9	3.7	107.5	2.2	−2013	25.5	−31.1	1.0	VLE
	0.1013	7.0	940.5	7.9	174.9	5.5	−1995	15.8	−49.4	2.1	VLE
313.75	0.4979	1.0	836.8	4.3	17.3	0.1	−1563	15.5	−4.9	0.1	VLE
	0.4993	3.0	843.0	5.1	56.5	0.6	−1471	21.0	−16.5	0.2	VLE
	0.4994	5.0	848.9	2.4	105.8	3.8	−1409	25.7	−30.8	1.3	VLE
	0.4996	7.0	858.8	6.4	180.4	13.9	−1341	9.2	−50.8	3.5	VLE
313.75	0.7477	1.0	792.5	6.2	17.2	0.2	−1317	11.2	−5.5	0.9	VLE
	0.7525	2.0	802.6	4.3	36.2	0.5	−1273	4.1	−11.7	2.4	VLE
	0.7486	3.0	808.4	7.3	58.3	1.2	−1209	5.5	−38.6	2.1	VLE
	0.7497	4.0	811.0	4.7	79.9	1.2	−1146	15.7	−23.1	0.6	VLE
	0.7497	5.0	824.3	7.6	104.9	2.0	−1082	14.6	−30.1	0.7	VLE
	0.7498	6.0	826.9	8.9	140.2	5.2	−1020	6.8	−39.9	1.2	VLE
	0.7512	7.0	834.1	6.3	182.0	7.8	−932	12.5	−53.7	5.5	VLE
313.75	1.0	1.0	759.8	3.7	17.3	0.4	−1127	7.1	−12.9	8.9	VLE
	1.0	1.5	765.2	6.0	26.6	0.2	−1094	21.1	−7.8	0.5	VLE
	1.0	2.0	770.4	3.7	36.5	0.2	−1047	11.2	−11.6	1.2	VLE
	1.0	3.0	779.9	4.8	56.7	1.9	−976	19.9	−26.0	18.8	VLE
	1.0	4.0	796.3	4.2	77.6	2.8	−911	13.2	−21.7	0.9	VLE
	1.0	5.0	801.0	3.2	107.4	1.2	−860	15.6	−31.0	0.4	VLE
354.35	0.0953	1.0	895.0	5.6	14.7	0.1	−1961	12.2	−4.8	0.5	VLE
	0.0980	3.0	897.5	2.1	47.6	0.3	−1933	8.5	−13.7	1.0	VLE
	0.0982	5.0	905.0	5.2	84.6	1.0	−1924	19.2	−23.2	0.8	VLE
	0.1012	7.0	906.0	9.3	127.5	3.2	−1876	21.9	−33.0	1.2	VLE
	0.1002	9.0	895.8	14.0	174.0	2.9	−1864	22.2	−46.5	2.3	VLE
354.35	0.4862	1.0	794.4	6.1	14.6	0.4	−1477	13.3	−10.2	2.5	VLE
	0.4945	3.0	800.0	2.9	46.8	1.2	−1412	7.1	−19.2	5.6	VLE
	0.4974	5.0	797.9	1.0	84.9	0.3	−1361	28.9	−24.1	0.9	VLE
	0.4981	7.0	804.7	5.4	127.0	2.1	−1330	36.7	−35.5	2.1	VLE
	0.4978	8.0	802.8	3.7	152.7	6.2	−1267	8.4	−43.8	1.5	VLE
354.35	0.7445	1.0	744.9	4.2	14.2	0.5	−1242	3.9	−14.6	7.7	VLE
	0.7515	2.0	749.7	2.7	30.5	0.5	−1209	8.4	−11.5	2.8	VLE
	0.7463	3.0	750.9	6.7	47.4	1.0	−1176	8.6	−16.3	3.2	VLE
	0.7541	4.0	753.8	1.7	65.7	0.4	−1137	17.6	−20.0	1.1	VLE
	0.7473	5.0	758.6	5.9	85.4	1.3	−1115	18.0	−27.3	3.0	VLE
	0.7572	6.0	762.5	5.1	106.1	3.4	−1069	15.7	−29.6	0.6	VLE
	0.7570	7.0	759.4	3.7	126.3	3.9	−1018	18.9	−37.9	5.7	VLE
	0.7576	8.0	763.2	2.8	154.5	13.6	−956	7.9	−42.5	5.5	VLE
354.35	1.0	1.0	706.6	4.1	14.8	0.2	−1066	7.6	−9.8	3.2	VLE
	1.0	1.5	713.3	5.8	22.5	0.5	−1055	10.1	−14.8	4.1	VLE
	1.0	2.0	710.8	4.8	31.2	1.0	−1023	4.9	−23.1	12.5	VLE
	1.0	2.5	718.0	3.4	39.0	0.6	−1006	5.9	−14.9	2.3	VLE
	1.0	3.0	719.2	5.7	49.0	2.6	−984	14.6	−23.4	12.0	VLE
	1.0	4.0	727.7	5.5	66.0	1.4	−958	8.6	−21.9	2.0	VLE
	1.0	5.0	726.8	5.2	85.1	2.3	−903	19.7	−27.8	4.4	VLE
	1.0	6.0	735.0	2.8	104.3	2.4	−864	15.5	−30.0	2.7	VLE
	1.0	7.0	733.0	10.4	739.9	19.0	−794	10.9	−766	49.9	LLE
395.0	0.0681	1.0	852.6	9.1	11.5	0.2	−1879	16.2	−17.9	4.1	VLE
	0.0886	3.0	846.5	2.5	39.8	0.5	−1825	12.9	−15.8	0.7	VLE
	0.0933	5.0	856.1	8.7	70.4	0.5	−1816	18.2	−22.1	2.4	VLE
	0.0954	7.0	852.6	8.6	103.1	1.7	−1781	19.2	−28.7	1.7	VLE
	0.0978	9.0	854.1	7.2	139.1	2.6	−1763	8.6	−41.4	2.7	VLE
395.0	0.4637	1.0	729.6	6.2	11.7	0.1	−1378	11.9	−21.1	2.2	VLE
	0.4740	3.0	737.7	7.9	40.7	1.3	−1332	16.4	−29.7	1.8	VLE
	0.4879	5.0	746.2	5.1	71.0	0.4	−1288	10.4	−28.0	2.0	VLE
	0.4934	7.0	739.1	5.2	106.1	3.2	−1227	13.1	−42.2	5.6	VLE
	0.4967	9.0	728.6	13.4	136.2	2.3	−1168	7.9	−40.2	4.2	VLE
395.0	0.7406	1.0	692.2	7.3	12.0	0.2	−1160	4.6	−28.3	5.9	VLE
	0.7348	2.0	691.6	7.2	26.3	0.7	−1129	17.4	−35.9	7.6	VLE
	0.7451	3.0	691.5	3.7	41.3	1.1	−1102	7.3	−31.0	6.6	VLE
	0.7469	4.0	695.9	4.1	56.2	1.5	−1070	18.6	−33.1	1.8	VLE
	0.7627	5.0	695.7	4.3	71.3	2.9	−1044	22.1	−41.9	10.9	VLE
	0.7446	6.0	700.7	6.5	89.4	1.4	−1027	24.2	−41.5	14.8	VLE
	0.7637	7.0	699.6	9.4	105.6	2.9	−987	18.0	−48.5	4.9	VLE

TABLE 3 (Continued)

T (K)	$\tilde{x}_M$ (mol/mol)	p (MPa)	ρ^I (kg/m^3)	$\Delta\rho^I$ (kg/m^3)	ρ^{II} (kg/m^3)	$\Delta\rho^{II}$ (kg/m^3)	u^I (kJ/kg)	Δu^I (kJ/kg)	u^{II} (kJ/kg)	Δu^{II} (kJ/kg)	state
395.0	1.0	1.0	649.6	8.5	12.4	0.5	−987	12.9	−63.1	5.7	VLE
	1.0	1.5	654.0	6.9	19.0	0.9	−979	8.7	−62.8	7.6	VLE
	1.0	2.0	661.7	4.6	27.7	1.1	−970	9.0	−64.3	13.5	VLE
	1.0	2.5	660.1	8.2	34.4	1.8	−951	12.8	−44.5	9.5	VLE
	1.0	3.0	664.5	6.2	42.2	1.4	−944	12.8	−39.4	13.0	VLE
	1.0	3.5	664.8	7.8	50.3	2.1	−928	14.4	−47.4	14.8	VLE
	1.0	4.0	666.7	4.8	57.6	2.3	−915	10.5	−43.8	10.0	VLE
	1.0	5.0	663.2	6.5	73.4	2.0	−878	15.1	−47.2	14.3	VLE
	1.0	6.0	660.7	6.3	91.8	4.5	−833	13.6	−49.8	16.1	VLE
	1.0	7.0	675.8	7.8	111.2	5.4	−836	21.1	−57.7	17.3	VLE

[a] The liquid and vapor phases are labeled by I and II, respectively.

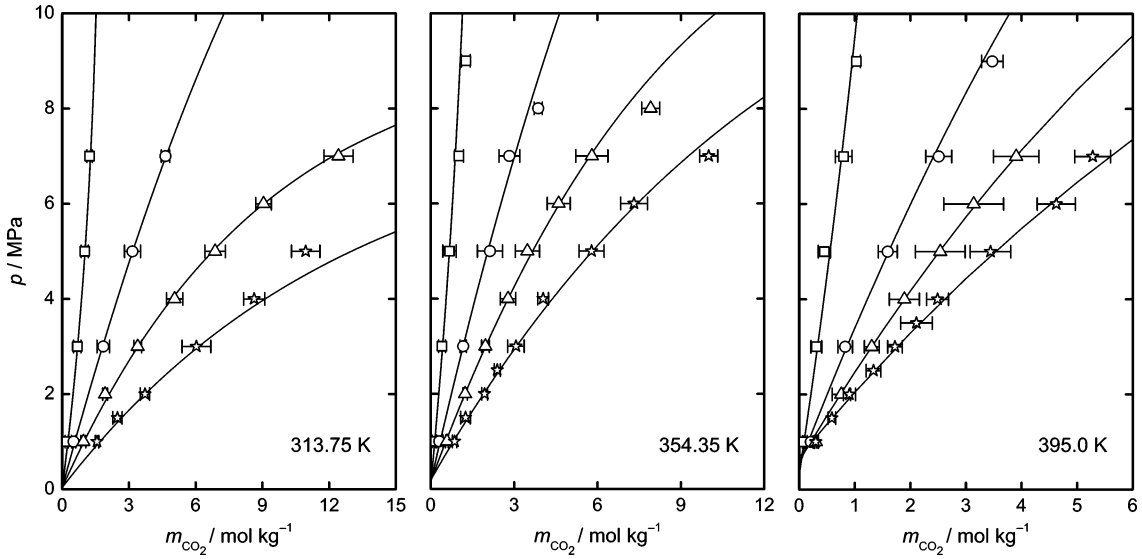

Figure 4. Solubility of CO_2 in aqueous solutions of methanol at 313.75, 354.35, and 395.0 K. Comparison between simulation results of this work (□ ($\bar{\tilde{x}}_M = 0.1$), ○ ($\bar{\tilde{x}}_M = 0.5$), △ ($\bar{\tilde{x}}_M = 0.75$), ☆ ($\bar{\tilde{x}}_M = 1.0$)) and experimental data of Xia et al.[24] (solid lines).

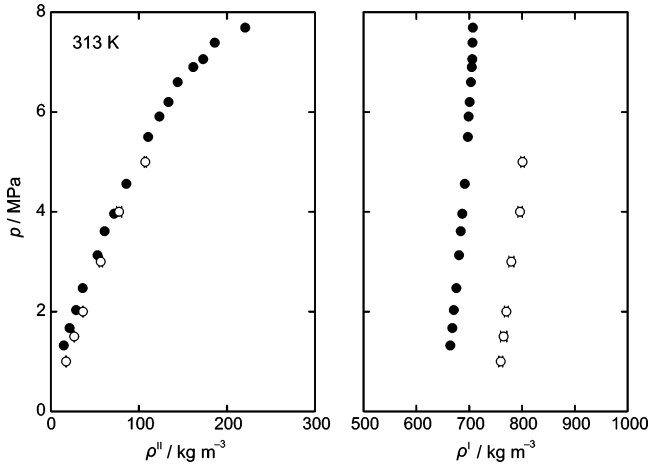

Figure 5. Densities of the coexisting phases in the binary system CO_2 and methanol at 313 K. Comparison between simulation results of this work (○) and experimental data of Chang et al.[25] (●).

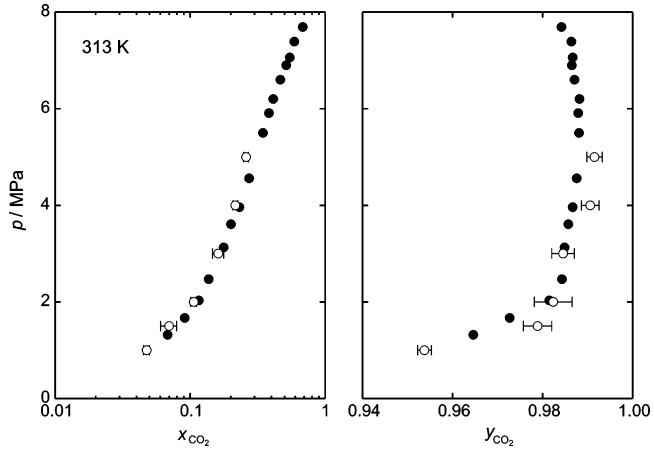

Figure 6. Pressure−composition diagram of the binary system CO_2 and methanol at 313 K. Comparison between simulation results of this work (○) and experimental data of Chang et al.[25] (●).

carbon dioxide in all investigated solvent mixtures amounts to 4.5% at 313.75 K, 5.1% at 354.35 K, and 7.8% at 395.0 K. Figures 5 and 6 show simulation results for the densities and the compositions of the coexisting phases in the binary carbon dioxide−methanol mixture at 313 K in comparison with the experimental data of Chang et al.[25] The predictions for the vapor-phase density agree well with the experimental values, whereas the simulation overestimates the liquid-phase density of the binary mixture by about 15%. As it is expected, the simulation results for the solubility of carbon dioxide in methanol agree well with that experimental data. The simulation results for the small concentrations of methanol in compressed carbon dioxide ($y_M = 1 - y_{CO_2} \approx 0.02$ mol/mol) also agree well with the experimental data. The maximum deviation amounts about twice the statistical uncertainties of the simulation results (cf. Figure 6). The simulation results for the density of the ternary carbon dioxide−methanol−water mixtures could not be compared to the experiments due to the lack of experimental data. In the liquid mixture, the residual part of the internal energy is

TABLE 4: Henry's Constant of Carbon Dioxide in (Water + Methanol) on the Molality Scale from Molecular Simulations of This Work and Experiments (cf. Ref 24)

	$T = 313.75$ K		$T = 354.35$ K		$T = 395.0$ K	
$\tilde{x}_M$	$\ln[k_{H,CO_2}^{(exp)}(MPa)]$	$\ln[k_{H,CO_2}^{(sim)}(MPa)]$	$\ln[k_{H,CO_2}^{(exp)}(MPa)]$	$\ln[k_{H,CO_2}^{(sim)}(MPa)]$	$\ln[k_{H,CO_2}^{(exp)}(MPa)]$	$\ln[k_{H,CO_2}^{(sim)}(MPa)]$
0.1	1.327 ± 0.007	1.602 ± 0.103	1.849 ± 0.006	1.984 ± 0.039	2.057 ± 0.006	2.325 ± 0.186
0.5	0.494 ± 0.008	0.505 ± 0.113	0.866 ± 0.004	0.919 ± 0.160	1.022 ± 0.005	1.195 ± 0.243
0.75	0.084 ± 0.004	-0.226 ± 0.230	0.495 ± 0.016	0.329 ± 0.170	0.703 ± 0.019	0.808 ± 0.110
1.0	-0.496 ± 0.017	-0.627 ± 0.130	0.009 ± 0.006	-0.036 ± 0.171	0.294 ± 0.004	0.601 ± 0.114

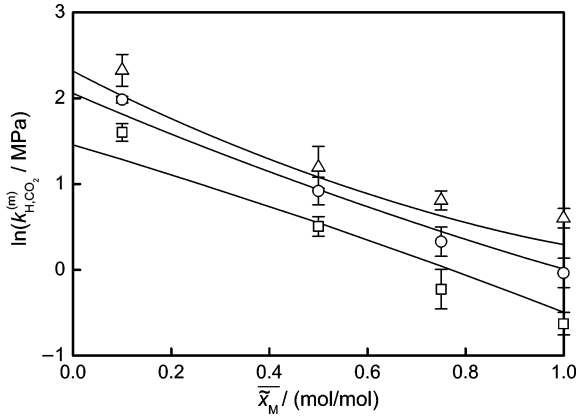

Figure 7. Henry's constant of CO_2 in (methanol + water) on the molality scale. Comparison between simulation results of this work (□ (313.75 K), ○ (354.35 K), △ (395.0 K)) and experimental data of Xia et al.[24] (solid lines).

dominated by contributions from electrostatic interactions, whereas in the vapor phase, the contributions from the Lennard-Jones interactions dominate the residual parts of the internal energy. Comparisons between simulation results and experimental data are desirable also for other properties (microscopic properties e.g., radial distribution functions as well as macroscopic (i.e., thermodynamic) properties). However, such comparisons cannot be performed because, to the best of our knowledge, no experimental data is available in the open literature.

The simulation results were also evaluated to determine Henry's constants (on the molality scale) for CO_2 in (CH_3OH + H_2O). The results are given in Table 4 and shown in Figure 7. As expected, the Henry's constant increases with increasing temperature, but decreases with increasing concentration of methanol in the solvent mixture. The average relative deviation between the simulation results and the experimental data (Xia et al.[24]) is 18% at 313.75 K, 10% at 354.35 K, and 27% at 395.0 K. These differences are in the same order of magnitude as often-encountered differences between experimental data from different groups.

5. Conclusions

Simulation results for the solubility of carbon dioxide at temperatures between 313 and 395 K in pure methanol and in aqueous solutions of methanol are presented and compared with recently published experimental data. Although no parameter for binary interactions was fitted to the experimental results for the solubility of carbon dioxide, the predicted results agree well with the experimental data, i.e., the deviations between simulation results and experimental data are of the same order of magnitude than the statistical uncertainty of the simulation results. The results of this study along with previous simulations for carbon dioxide in water[18] and for high-pressure equilibrium of the system carbon dioxide−methanol−water[1] confirm that molecular simulation is a good tool for reliable estimation of gas solubilities in mixed solvent systems.

Acknowledgment. We appreciate the support from the Regionales Hochschulrechenzentrum Kaiserslautern (RHRK) which provided CPU time on its supercomputers as well as financial support by the Deutsche Forschungsgemeinschaft (DFG).

References and Notes

(1) Kristóf, T.; Vorholz, J.; Maurer, G. *J. Phys. Chem. B* **2002**, *106*, 7547.
(2) Potoff, J. J.; Errington, J. R.; Panagiotopoulos, A. Z. *Mol. Phys.* **1999**, *97*, 1073.
(3) Palinkas, G.; Hawlicka, E.; Heinzinger, K. *Chem. Phys.* **1991**, *158*, 65.
(4) Ferrario, M.; Haughney, M.; McDonald, I. R.; Klein, M. L. *J. Chem. Phys.* **1990**, *93*, 5156.
(5) Strauch, H. J.; Cummings, P. T. *Fluid Phase Equilib.* **1993**, *83*, 213.
(6) Strauch, H. J.; Cummings, P. T. *Fluid Phase Equilib.* **1993**, *86*, 147.
(7) Haughney, M.; Ferrario, M.; McDonald, I. R. *J. Phys. Chem.* **1987**, *91*, 4934.
(8) Handgraaf, J. W.; Meijer, E. J.; Gaigeot, M. P. *J. Chem. Phys.* **2004**, *121*, 10111.
(9) Venables, D. S.; Schmuttenmaer, C. A. *J. Chem. Phys.* **2000**, *113*, 11222.
(10) Laaksonen, A.; Kusalik, P. G.; Svishchev, I. M. *J. Phys. Chem. A* **1997**, *101*, 5910.
(11) Weerasinghe, S.; Smith, P. E. *J. Phys. Chem. B* **2005**, *109*, 15080.
(12) Stubbs, J. M.; Siepmann, J. I. *J. Chem. Phys.* **2004**, *121*, 1525.
(13) Panagiotopoulos, A. Z. *Mol. Phys.* **1987**, *61*, 813.
(14) Panagiotopoulos, A. Z.; Quirke, N.; Stapleton, M.; Tildesley, D. J. *Mol. Phys.* **1988**, *63*, 527.
(15) Harris, J. G.; Yung, K. H. *J. Phys. Chem.* **1995**, *99*, 12021.
(16) Berendsen, H. J. C.; Postma, J. P. M.; van Gunsteren, W. F.; Hermans, J. In *Intermolecular Forces*; Pullmann, B., Ed.; Reidel: Dordrecht, The Netherlands, 1981; p 331.
(17) van Leeuwen, M. E.; Smit, B. *J. Phys. Chem.* **1995**, *99*, 1831.
(18) Vorholz, J.; Harismiadis, V. I.; Rumpf, B.; Panagiotopoulos, A. Z.; Maurer, G. *Fluid Phase Equilib.* **2000**, *170*, 203.
(19) Errington, J. R.; Panagiotopoulos, A. Z. *J. Phys. Chem. B* **1998**, *102*, 7470.
(20) Theodorou, D. N.; Suter, U. W. *J. Chem. Phys.* **1985**, *82*, 955.
(21) Allen, M. P.; Tildesley, D. J. *Computer Simulation of Liquids*; Clarendon Press: Oxford, U. K., 1987.
(22) de Leeuw, S. W.; Perram, J. W.; Smith, E. R. *Proc. R. Soc. London Ser. A* **1980**, *A373*, 27.
(23) Pérez-Salado Kamps, Á. *Ind. Eng. Chem. Res.* **2005**, *44*, 201.
(24) Xia, J.; Jödecke, M.; Pérez-Salado Kamps, Á.; Maurer, G. *J. Chem. Eng. Data* **2004**, *49*, 1756.
(25) Chang, C. J.; Day, C.-Y.; Ko, C.-M.; Chiu, K.-L. *Fluid Phase Equilib.* **1997**, *131*, 243.